



# Reflection of Plane Waves in a Transversely Isotropic Rotating Microstretch Elastic Half-Space

Princy Gupta\* and Jitander Singh Sikka

Department of Mathematics, Maharshi Dayanand University, Rohtak, India

\*Corresponding author: [princygupta31394@gmail.com](mailto:princygupta31394@gmail.com)

Received: March 26, 2023

Accepted: May 1, 2023

**Abstract.** In this paper, the impact of rotation on the propagation of plane waves for various rotation parameter values has been studied. For this purpose, a model has been developed which is assumed to rotate with uniform angular velocity. A transversely isotropic solid medium with microstretch elastic properties has linear governing equations that are focused in the  $x$ - $z$  plane. For the incident *Coupled Longitudinal Displacement (CLD)* wave, four reflected coupled plane waves exist in the same medium. A half-space surface with no stresses of a material is thought to exist where the *CLD* wave reflects. On the stress-free surface of the half-space, the appropriate potentials for the incident and reflected waves satisfy the necessary boundary conditions, and relationships in the amplitude ratios of reflected waves are obtained. Graphs of plane wave speeds and amplitude ratios versus propagation angle are shown for various values of the rotation parameter.

**Keywords.** Plane waves, Rotation, Microstretch elastic half-space, Amplitude ratios

**Mathematics Subject Classification (2020).** 104A58, 104A66

Copyright © 2023 Princy Gupta and Jitander Singh Sikka. *This is an open access article distributed under the Creative Commons Attribution License, which permits unrestricted use, distribution, and reproduction in any medium, provided the original work is properly cited.*

## 1. Introduction

### 1.1 Background

In a mathematical sense, continuum materials are addressed by classical elasticity theory. In this continuum, the molecular structure of the material is disregarded and its points are thought of as material particles, which are just geometrical points in three-dimensional Euclidean spaces. Some materials, such as steel, aluminium, concrete, etc., are found to exhibit results that fairly coincide with those of experimentally observed results when they are within

the elastic limits. There are notable discrepancies between experimental results and those obtained using classical elasticity in some materials, such as fibrous materials, polymers, and asphalts. These differences are primarily caused by the predominance of the atomic structures of the materials, which were ignored in classical elasticity. These discrepancies are readily apparent when it comes to dynamical difficulties with elastic vibrations involving high frequencies and brief wavelengths, or ultrasonic waves. When granular and multi-molecular bodies vibrate, new types of waves that were not anticipated by the classical theory of elasticity appear, making the influence of microstructure more significant. The theories of “micropolar continua” and “microstretch continua”, which are specialized versions of the theory of “micromorphic continua” that Eringen and his collaborators had previously developed, were created by Eringen in 1967 and 1990, respectively. So, the “3M” theories of Eringen (Micromorphic, Microstretch and Micropolar) are the generalization of the traditional theory of elasticity. In the theory of polar continuum mechanics, every material point possesses a unique deformable microstructure. The terms “classical macrodeformation” and “microdeformation” describe the deformation of a particle in a micromorphic continuum (microrotation of directors and microstretch of directors). Each point can experience microrotation and microstretch (breathing micromotion) during a micro stretch continuum’s deformation process without experiencing microshearing or breathing microrotation. Three translational, three microrotational, and one rotational degree of freedom make up the seven degrees of freedom in microstretch bodies.

## 1.2 Literature Review

Eringen was the first to develop a description of the micropolar fluids and microstretch elastic body theory [2, 3]. Based on the concept of microstretch elasticity developed by Eringen, many researchers have examined various issues. Isothermal bending of microstretch elastic plate was studied by Ciarletta [1]. Microstretch elastic solids’ equilibrium theory was studied by Iesan and Pompei [4]. In a microstretch solid, Kumar *et al.* [6] investigated the plane strain problem. Utilizing plate vibration data, Kiris and Inan [5] calculated the microstretch elastic moduli of various materials. Marin [7] developed the idea of domain of influence of microstretch materials. Many authors have researched various issues relating to plane waves and surface waves in isotropic microstretch elastic materials. For instance, in his study of the movement of a microrotation and microstretch wave in a nonlocal medium, Nowinski [8] also specialized the general field equations governing the movement of a nonlocal surface wave. Sharma *et al.* [10] took into account the issues with Rayleigh surface wave propagation in an isotropic microstretch continua with effects of micropolarity and relaxation times. The plane waves in an isotropic electromicrostretch elastic solid were investigated by Sharma *et al.* [9]. At a microstretch solid/fluid interface, Singh *et al.* [12] took into account the reflection and transmission of dilatation waves. Singh and Goyal [11] solved the problem for plane wave propagation in transversely isotropic microstretch elastic solid and computed the speeds and reflection coefficients of reflected waves.

### 1.3 Contribution

The objective of the present paper is to conduct an investigation how rotation affects the propagation of plane waves in a transversely isotropic microstretch medium. The graphs of speeds and amplitude ratios are drawn against the angle of propagation for different values of rotation parameter and the variations of speeds and amplitude ratios are compared when rotation is present and absent.

### 1.4 Structure of the Paper

This paper is organised as follows: Basic equations of motion are taken in Section 2. These fundamental equations are developed and solved for plane wave solutions in Section 3. Section 4 is the reflection from stress free surface. Results are discussed in Section 5 and, conclusions are drawn in Section 6.

## 2. Governing Equations

We consider a homogeneous transversely isotropic microstretch solid half-space which rotates uniformly with angular velocity

$$\Omega = \Omega \hat{n},$$

where  $\Omega$  is a rotation parameter and  $\hat{n}$  is a unit vector representing the direction of axis of rotation.

### 2.1 Equations of Motion

The following equations make up the linear theory of microstretch elasticity:

$$t_{ji,j} = \rho[u_i + \{\Omega \times (\Omega \times u)\}_i + (2\Omega \times u)_i], \tag{2.1}$$

$$m_{ik,i} + \epsilon_{ijk} t_{ij} = \rho j \ddot{\phi}_k, \tag{2.2}$$

$$\pi_{k,k} - \sigma = j_0 \ddot{\phi}_k. \tag{2.3}$$

### 2.2 The Constitutive Equations

$$t_{ij} = A_{ijrs} e_{rs} + B_{ijrs} \kappa_{rs} + D_{ij} \Phi + F_{ijk} \gamma_k, \tag{2.4}$$

$$m_{ij} = B_{rsij} e_{rs} + C_{ijrs} \kappa_{rs} + E_{ij} \Phi + G_{ijk} \gamma_k, \tag{2.5}$$

$$\sigma = D_{ij} e_{ij} + E_{ij} \kappa_{ij} + \gamma \Phi + h_k \gamma_k, \tag{2.6}$$

$$\pi_k = F_{ijk} e_{ij} + G_{ijk} \kappa_{ij} + h_k \phi + A_{kj}^* \gamma_j, \tag{2.7}$$

$$e_{ij} = u_{j,i} + \epsilon_{ijk} \phi_k, \quad \kappa_{ij} = \phi_{j,i}, \quad \gamma_j = \Phi_{,j}, \tag{2.8}$$

Here, the force stress tensor is  $t_{ij}$ , the couple stress tensor is  $m_{ij}$ , the density is  $\rho$ , the components of the displacement vector are  $u_i$ , the alternating tensor is  $\epsilon_{ijk}$  and the components of the microrotation vector are  $\phi_i$ . The microstretch function is represented by  $\pi_k$ , the microstress function  $\Phi$ , the microinertia by  $\sigma$ , the microinertia by  $j$ , the microstretch inertia by  $j_0$ . The kinematic strain measures are  $e_{ij}$ ,  $\kappa_{ij}$  and  $\zeta_k$  and constitutive coefficients are  $A_{ijrs}$ ,  $B_{ijrs}$ ,  $C_{ijrs}$ ,  $D_{ij}$ ,  $E_{ij}$ ,  $F_{ijk}$ ,  $G_{ijk}$ ,  $h_i$ ,  $A_{ij}$ ,  $\kappa_{ij}$ . Latin subscripts cover the entire range of integers (1,2,3). Commas before subscripts indicate partial differentiation in relation to

the corresponding Cartesian coordinates. A superposed dot indicates partial differentiation with respect to time  $t$ . The following symmetry relations are taken to hold for the constitutive coefficients and the microinertia tensor.

$$A_{ijrs} = A_{rsij}, \quad B_{ijrs} = B_{rsij}, \quad C_{ijrs} = C_{rsij}, \quad A_{ij} = A_{ji}, \quad \kappa_{ij} = \kappa_{ji}. \tag{2.9}$$

### 3. Formulation of the Problem and Plane Wave Solutions

We take into account a rotating transversely isotropic micostretch elastic solid half-space. When we consider the free surface as the origin of coordinate system, the negative  $z$  axis is seen to be pointing normally into the half-space, which is denoted by the symbol  $z \leq 0$ . We believe that the medium is transversely isotropic in the sense that the isotropic planes are perpendicular to the  $z$ -axis.

$$u = (u_1, 0, u_3) \quad \text{and} \quad \phi = (0, \phi_2, 0).$$

Using equations (2.4) to (2.9) in equations (2.1) to (2.3), we obtain

$$A_{11} \frac{\partial^2 u_1}{\partial x^2} + (A_{13} + A_{56}) \frac{\partial^2 u_3}{\partial x \partial z} + A_{55} \frac{\partial^2 u_1}{\partial z^2} + K_1 \frac{\partial \phi_2}{\partial z} + D_{11} \frac{\partial \Phi}{\partial x} = \rho \left[ \frac{\partial^2 u_1}{\partial t^2} - \Omega^2 u_1 + 2\Omega \frac{\partial u_3}{\partial t} \right], \tag{3.1}$$

$$A_{66} \frac{\partial^2 u_3}{\partial x^2} + (A_{13} + A_{56}) \frac{\partial^2 u_1}{\partial x \partial z} + A_{33} \frac{\partial^2 u_3}{\partial z^2} + K_2 \frac{\partial \phi_2}{\partial x} + D_{33} \frac{\partial \Phi}{\partial z} = \rho \left[ \frac{\partial^2 u_3}{\partial t^2} - \Omega^2 u_3 - 2\Omega \frac{\partial u_1}{\partial t} \right], \tag{3.2}$$

$$B_{77} \frac{\partial^2 \phi_2}{\partial x^2} + B_{66} \frac{\partial^2 \phi_2}{\partial z^2} - K_1 \frac{\partial u_1}{\partial z} - K_2 \frac{\partial u_3}{\partial x} - \chi \phi_2 = \rho j \frac{\partial^2 \phi_2}{\partial t^2}, \tag{3.3}$$

$$A_{11}^* \frac{\partial^2 \Phi}{\partial x^2} + A_{33}^* \frac{\partial^2 \Phi}{\partial z^2} - \zeta \Phi - D_{11} \frac{\partial u_1}{\partial x} - D_{33} \frac{\partial u_3}{\partial z} = j_0 \frac{\partial^2 \Phi}{\partial t^2}. \tag{3.4}$$

We seek the plane wave solutions of equations (3.1) to (3.4) as follows:

$$\{u_1, u_3, \phi_2, \Phi\} = \{A, B, C, D\} \exp\{ik(x \sin \theta + z \cos \theta - vt)\}, \tag{3.5}$$

where  $\omega = kv$  is the angular frequency,  $\theta$  is the angle of wave propagation direction with vertical axis,  $k$  is the wave number, and  $v$  is wave speed.

We achieve four homogeneous equations in  $A, B, C$ , and  $D$  that have a non-trivial solution if equation (3.5) is used in equations (3.1) to (3.4),

$$A^* \Lambda^4 - B^* \Lambda^3 + C^* \Lambda^2 - D^* \Lambda + E^* = 0, \tag{3.6}$$

where

$$\Lambda = \rho v^2,$$

$$A^* = P^2 + Q^2,$$

$$B^* = P(D_1 + D_2) + P^2(D_3^* + D_4^*) + Q^2(D_3^* + D_4^*),$$

$$C^* = D_1 D_2 + P(D_1 D_3^* + D_2 D_3^* + D_1 D_4^* + D_2 D_4^*) + P^2 D_3^* D_4^* + Q^2 D_3^* D_4^* - P(D_{11} D_{11}^* \sin^2 \theta + K_1 K_1^* \cos^2 \theta + D_{33} D_{33}^* \cos^2 \theta + K_2 K_2^* \sin^2 \theta) + Q(D_{11} D_{33}^* \sin \theta \cos \theta - i D_{33} D_{11}^* \sin \theta \cos \theta) - L^2,$$

$$D^* = D_1 D_2 D_3^* + D_1 D_2 D_4^* + P(D_1 D_3^* D_4^* + D_2 D_3^* D_4^*) - [P(D_{11} D_{11}^* D_3^* + K_2 K_2^* D_4^*) + D_{11} D_{11}^* D_2 + K_2 D_1^* K_2^*] \sin^2 \theta - [P(D_{33} D_{33}^* D_3^* + K_1 K_1^* D_4^*) + D_{33} D_{33}^* D_1]$$

$$\begin{aligned}
 &+ K_1 D_2 K_1^*] \cos^2 \theta + L(D_{11} D_{33}^* + K_1 K_2^* + K_2 K_1^* + D_{11}^* D_{33}) \sin \theta \cos \theta - 2(D_3^* + D_4^*), \\
 E^* = &D_1 D_2 D_3^* D_4^* - (D_{11} D_{11}^* D_2 D_3^* + K_2 K_2^* D_1 D_4^*) \sin^2 \theta - (K_1 K_1^* D_2 D_4^* + D_1 D_3^* D_{33} D_{33}^*) \cos^2 \theta \\
 &+ L(D_{11} D_{33}^* D_3^* + K_1 K_2^* D_4^* + K_2 K_1^* D_4^* + D_{11}^* D_{33} D_3^*) \sin \theta \cos \theta - (K_1 K_2^* D_{11}^* D_{33} \\
 &+ K_1^* K_2 D_{11} D_{33}^*) \sin^2 \theta \cos^2 \theta + K_1 K_1^* D_{33} D_{33}^* \cos^4 \theta + K_2 K_2^* D_{11} D_{11}^* \sin^4 \theta - L^2 (D_3^* D_4^*),
 \end{aligned}$$

where

$$D_1 = A_{11} \sin^2 \theta + A_{55} \cos^2 \theta, \quad D_2 = A_{66} \sin^2 \theta + A_{33} \cos^2 \theta, \quad D_3 = B_{77} \sin^2 \theta + B_{66} \cos^2 \theta,$$

$$D_4 = A_{11}^* \sin^2 \theta + A_{33}^* \cos^2 \theta, \quad L = (A_{13} + A_{56}) \sin \theta \cos \theta, \quad D_{11}^* = \frac{D_{11}}{j_0 k^2},$$

$$D_{33}^* = \frac{D_{33}}{\bar{j}_0 k^2}, \quad K_1^* = \frac{K_1}{j k^2}, \quad K_2^* = \frac{K_2}{j k^2},$$

$$D_3^* = \frac{D_3}{j} + \frac{\chi}{j k^2}, \quad D u^* = \frac{D u}{\bar{j}_0} + \frac{\xi}{\bar{j}_0 k^2}, \quad \bar{j}_0 = \frac{j_0}{\rho},$$

$$\Omega^* = \frac{\Omega}{k v}, \quad P = 1 + \Omega^{*2}, \quad Q = 2i \Omega^*.$$

The four roots of equation (3.6) shows the speed of propagation of *Coupled Longitudinal Displacement (CLD)* wave, *Coupled Longitudinal Microstretch (CLM)* wave, *Coupled Transverse Displacement (CTD)* wave and *Coupled Transverse Microrotational (CTM)* wave.

### 4. Reflection from a Stress Free Surface

The mechanical boundary condition, which includes the normal components of force stress, the tangential components of force stress, the tangential components of couple stress and the microstretch function, all vanish at  $z = 0$ .

$$t_{33} = 0, \quad t_{31} = 0, \quad m_{32} = 0, \quad \pi_3 = 0, \tag{4.1}$$

where

$$\begin{aligned}
 t_{33} = &A_{13} u_{1,1} + A_{33} u_{3,3} + D_{33} \Phi, \quad t_{31} = A_{56} u_{3,1} + A_{55} u_{1,3} + K_1 \Phi_2, \quad m_{32} = B_{66} \phi_{2,3}, \\
 \pi_3 = &h_3 \Phi + A_{31}^* \Phi_{,1} + A_{33}^* \Phi_{,3}.
 \end{aligned}$$

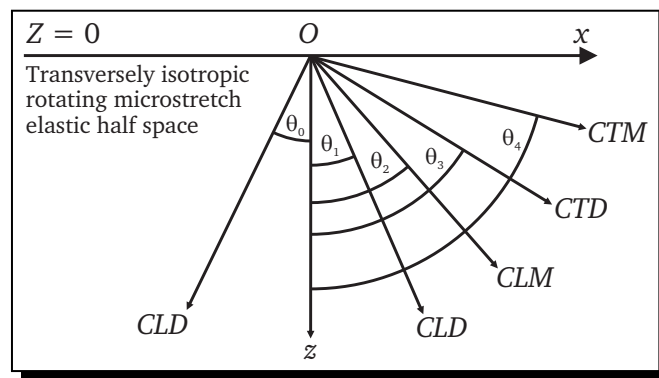


Figure 1. Geometrical representation

The appropriate displacement components  $u_1, u_3$ , microrotation vector  $\phi_2$  and microstress function  $\Phi$  are taken as

$$u_1 = A_0 \exp\{ik_1(x \sin \theta_0 + z \cos \theta_0 - v_1 t)\} + \sum_{j=1}^4 A_j \exp\{ik_j(x \sin \theta_j + z \cos \theta_j - v_j t)\}, \quad (4.2)$$

$$u_3 = p_1 A_0 \exp\{ik_1(x \sin \theta_0 + z \cos \theta_0 - v_1 t)\} + \sum_{j=1}^4 p_j A_j \exp\{ik_j(x \sin \theta_j + z \cos \theta_j - v_j t)\}, \quad (4.3)$$

$$\phi_2 = q_1 A_0 \exp\{ik_1(x \sin \theta_0 + z \cos \theta_0 - v_1 t)\} + \sum_{j=1}^4 q_j A_j \exp\{ik_j(x \sin \theta_j + z \cos \theta_j - v_j t)\}, \quad (4.4)$$

$$\Phi = r_1 A_0 \exp\{ik_1(x \sin \theta_0 + z \cos \theta_0 - v_1 t)\} + \sum_{j=1}^4 r_j A_j \exp\{ik_j(x \sin \theta_j + z \cos \theta_j - v_j t)\}, \quad (4.5)$$

where  $v_i$  ( $i = 1, 2, 3, 4$ ) are the actual velocity of the *CLD*, *CTD*, *CLM*, and *CTM* waves, respectively. These displacement components, the microrotation component, and the microstress function fulfill the boundary requirements (4.1) if following Snell's law hold.

$$k_1 \sin \theta_0 = k_1 \sin \theta_1 = k_2 \sin \theta_2 = k_3 \sin \theta_3 = k_4 \sin \theta_4, \quad (4.6)$$

$$k_1 v_1 = k_2 v_2 = k_3 v_3 = k_4 v_4 \quad (4.7)$$

and four equations in reflection coefficients are derived as a non-homogeneous system,

$$\sum_{j=1}^4 a_{ij} Z_j = b_i, \quad i = 1, 2, \dots, 4, \quad (4.8)$$

where

$$Z_j = \frac{A_j}{A_0}, \quad j = 1, 2, \dots, 4$$

are amplitude ratios of reflected *CLD*, *CTD*, *CTM* and *CLM* waves respectively, and

$$a_{1j} = \frac{iA_{13} \sin \theta_0 - ip_j A_{33} \left(\frac{v_1}{v_j}\right) \sqrt{1 - \sin^2 \theta_0 \left(\frac{v_j}{v_1}\right)^2} + D_{33} \left(\frac{r_j}{k_1}\right)}{iA_{13} \sin \theta_0 + ip_1 A_{33} \cos \theta_0 + D_{33} \frac{r_1}{k_1}}, \quad j = 1, 2, \dots, 4, \quad (4.9)$$

$$a_{2j} = \frac{ip_j A_{56} \sin \theta_0 - iA_{55} \left(\frac{v_1}{v_j}\right) \sqrt{1 - \sin^2 \theta_0 \left(\frac{v_j}{v_1}\right)^2} + K_1 \left(\frac{q_j}{k_1}\right)}{ip_1 A_{56} \sin \theta_0 + iA_{55} \cos \theta_0 + K_1 \frac{q_1}{k_1}}, \quad j = 1, 2, \dots, 4, \quad (4.10)$$

$$a_{3j} = \frac{q_j \left(\frac{v_1}{v_j}\right) \sqrt{1 - \sin^2 \theta_0 \left(\frac{v_j}{v_1}\right)^2}}{q_1 \cos \theta_0}, \quad j = 1, 2, \dots, 4, \quad (4.11)$$

$$a_{4j} = \frac{ir_j A_{31}^* \sin \theta_0 - ir_j A_{33}^* \left(\frac{v_1}{v_j}\right) \sqrt{1 - \sin^2 \theta_0 \left(\frac{v_j}{v_1}\right)^2} + h_3 \left(\frac{r_j}{k_1}\right)}{ir_1 A_{31}^* \sin \theta_0 + ir_1 A_{33}^* \cos \theta_0 + h_3 \frac{r_1}{k_1}}, \quad j = 1, 2, \dots, 4, \tag{4.12}$$

$$b_1 = -1, \quad b_2 = -1, \quad b_3 = 1, \quad b_4 = -1. \tag{4.13}$$

The above theoretical analysis minimizes to transversely isotropic microstretch elastic case when  $\Omega^* = 0, P = 1, Q = 0$ . The analysis cited above also boils down to transversely isotropic micropolar elastic case when  $\Omega^* = 0, P = 1, Q = 0, D_{11} = 0, D_{33} = 0$ .

## 5. Results and Discussion

In this study, the physical constants of a transversely isotropic composite material that is modelled as a microstretch medium are used to calculate plane wave speeds and reflection coefficients of reflected waves while meeting the inequalities between these constants:

$$\begin{aligned} A_{11} &= 17.8 * 10^{11} \text{ Nm}^{-2}, & A_{33} &= 18.43 * 10^{11} \text{ Nm}^{-2}, & A_{13} &= 7.59 * 10^{11} \text{ Nm}^{-2}, \\ A_{56} &= 1.89 * 10^{11} \text{ Nm}^{-2}, & A_{55} &= 4.357 * 10^{11} \text{ Nm}^{-2}, & A_{66} &= 4.42 * 10^{11} \text{ Nm}^{-2}, \\ A_{65} &= 4.32 * 10^{11} \text{ Nm}^{-2}, & B_{77} &= 0.278 * 10^{10} \text{ Nm}^{-2}, & B_{66} &= 0.268 * 10^{10} \text{ Nm}^{-2}, \\ A_{11}^* &= 0.03 * 10^{11} \text{ Nm}^{-2}, & A_{33}^* &= 0.04 * 10^{11} \text{ Nm}^{-2}, & D_{11} &= 0.062 * 10^{10} \text{ Nm}^{-2}, \\ D_{33} &= 0.063 * 10^{10} \text{ Nm}^{-2}, & \rho &= 1.74 * 10^3 \text{ Nm}^{-2}, & j &= 0.196 \text{ m}^2. \end{aligned}$$

For the above physical constants, the biquadratic equation (3.6) is solved mathematically for the phase speeds of the plane waves and equation (4.8) is also solved numerically to calculate the amplitude ratios of all reflected waves for different values of rotation rate.

### 5.1 Speeds of Plane Waves

The speeds of reflected *CLD*, *CTD*, *CLM* and *CTM* waves are plotted in Figures 2-5 versus the angle of incidence  $\theta_0$ , respectively. The red, green and blue lines of reflected waves corresponds to  $\Omega^* = 0, 0.1$  and  $0.2$ , respectively.

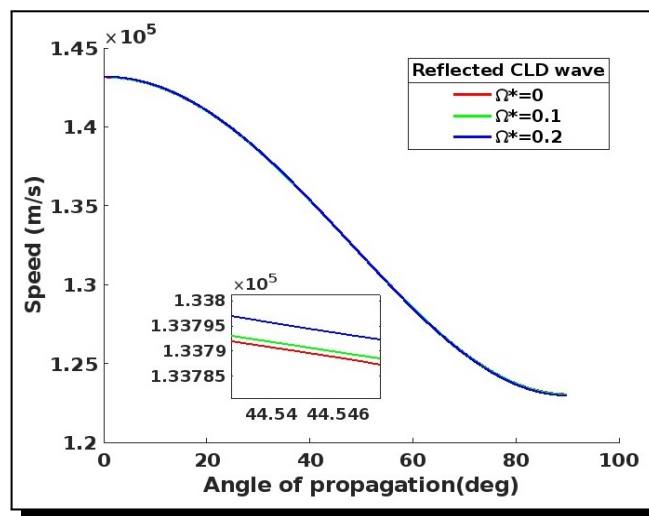


**Figure 2.** Speed of *CLD* wave versus angle of propagation for various values of rotation parameter

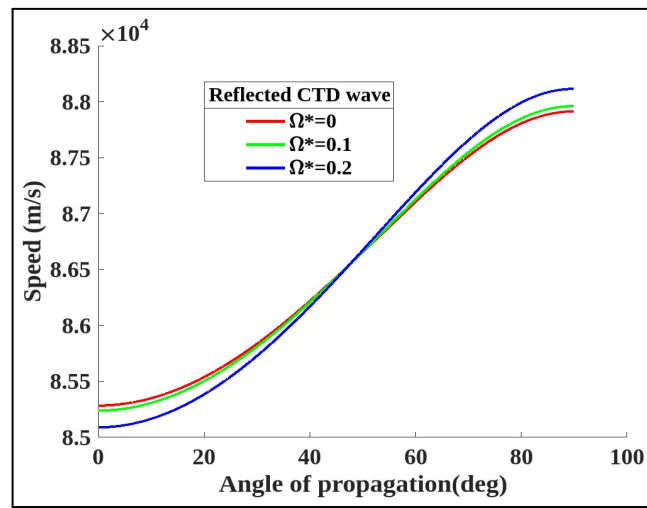


**Figure 3.** Speed of *CTD* wave versus angle of propagation for various values of rotation parameter

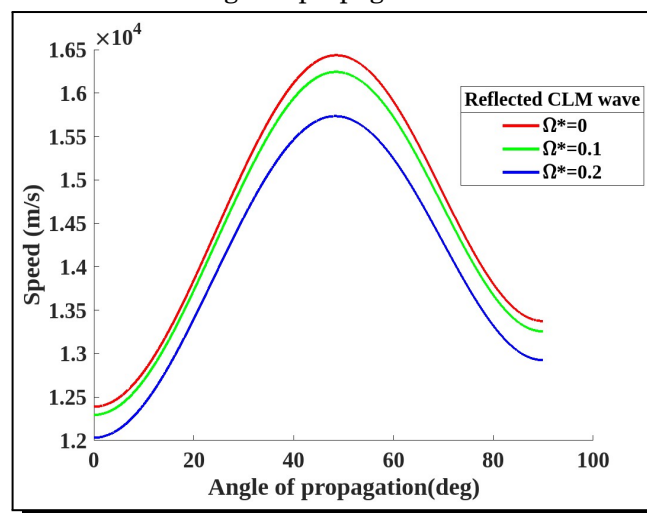


**Figure 4.** Speed of *CLM* wave versus angle of propagation for various values of rotation parameter

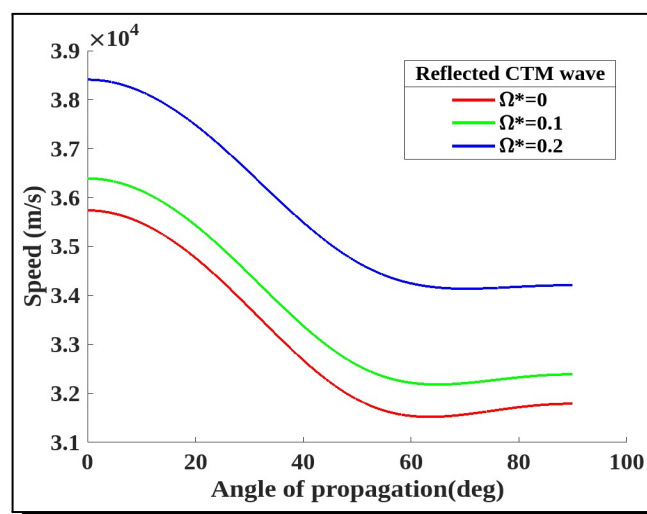


**Figure 5.** Speed of *CTM* wave versus angle of propagation for various values of rotation parameter

When  $\Omega^* = 0$ ,

- (a) the speed of the reflected *CLD* wave decreases monotonically from 141738 m/s at  $\theta_0 = 0$  to 121845 m/s at  $\theta_0 = 89.433$ ;
- (b) the speed of the reflected *CTD* wave increases monotonically from 85260.5 m/s at  $\theta_0 = 0$  to 87951.4 m/s at  $\theta_0 = 89.9544$ ;
- (c) the speed of the reflected *CLM* wave increases monotonically from 12383.4 m/s at  $\theta_0 = 0$  to 16431.6 m/s at  $\theta_0 = 48.6498$  and then decreases monotonically to the value 13372.4 m/s at  $\theta_0 = 89.7653$ ;
- (d) the speed of the reflected *CTM* wave decreases monotonically from 35731.9 m/s at  $\theta_0 = 0$  to its minimum value 31515.2 m/s at  $\theta_0 = 64.4635$  and then increases slowly upto the value 31783 m/s at  $\theta_0 = 90$ .

When rotation is present, (i.e. for  $\Omega^* = 0.1$  and  $0.2$ ), the speed variations of all reflected waves are similar to that for  $\Omega^* = 0$  for the corresponding wave, but the values of the speed enhance at each incident angle.

### 5.2 Amplitude Ratios of Plane Waves

Amplitude ratio versus angle of incidence  $\theta_0$  of reflected *CLD*, *CTD*, *CLM* and *CTM* waves are plotted in Figures 6-9, respectively. The red, green and blue lines of reflected waves corresponds to  $\Omega^* = 0, 0.1, 0.2$ , respectively.

When  $\Omega^* = 0$ ,

- (a) the amplitude ratio of the reflected *CLD* wave increases gradually from 2.02537 at  $\theta_0 = 42.6624$  and then increases to the value 1.01725 at  $\theta_0 = 89.4444$ .
- (b) the amplitude ratio of the reflected *CTD* wave gradually increases from 1.77854 at  $\theta_0 = 0$  to 1.87543 at  $\theta_0 = 36.4$  and subsequently decreases up to the value  $\theta_0 = 89.7023$ ;

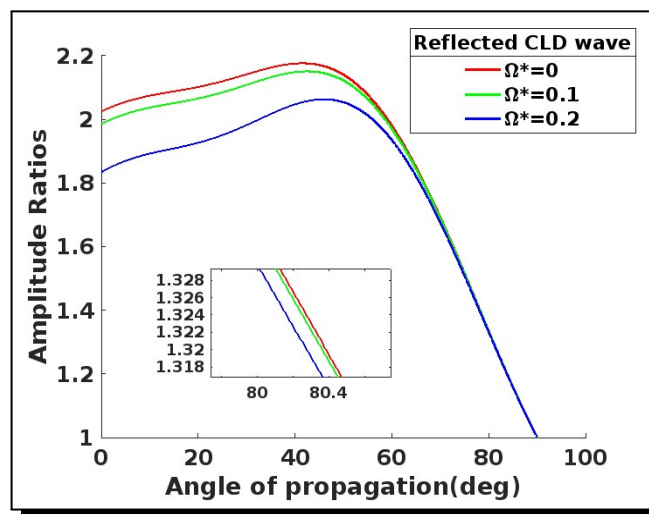


**Figure 6.** Amplitude ratio of *CLD* wave versus angle of propagation for various values of rotation parameter

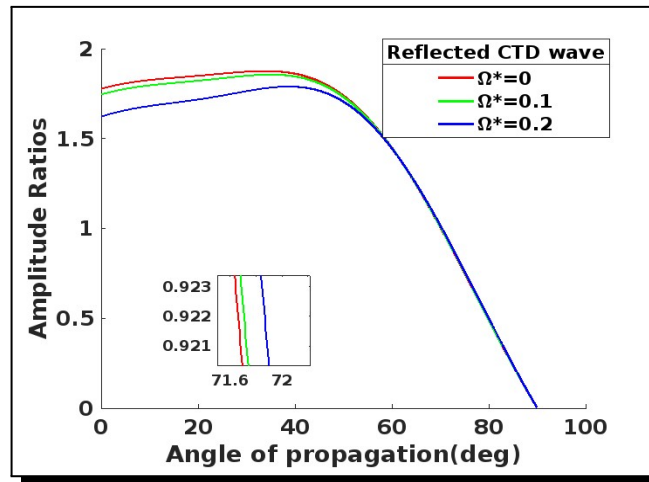


Figure 7. Amplitude ratio of CTD wave versus angle of propagation for various values of rotation parameter

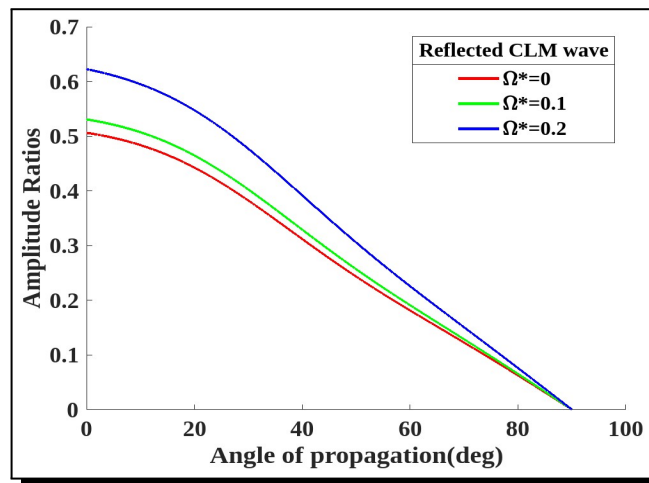


Figure 8. Amplitude ratio of CLM wave versus angle of propagation for various values of rotation parameter

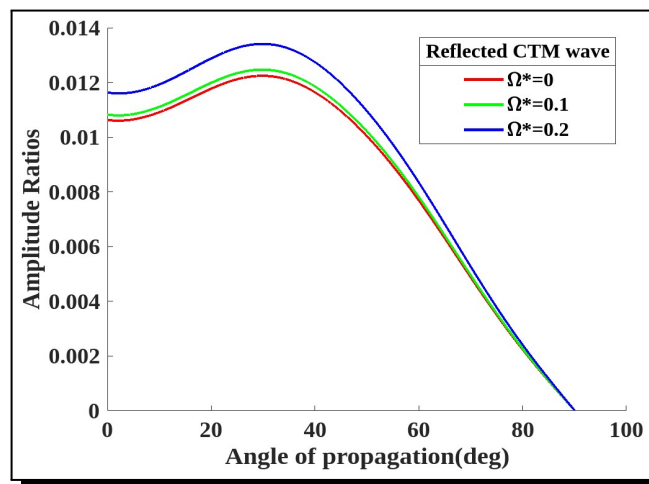


Figure 9. Amplitude ratio of CTM wave versus angle of propagation for various values of rotation parameter

- (c) the amplitude ratio of the reflected *CLM* wave gradually increases from 0.01062 at  $\theta_0 = 0.00572952$  to 0.0122211 at  $\theta_0 = 31.358$  and then declines to the value 0 at  $\theta_0 = 889.7997$ ;
- (d) the amplitude ratio of the reflected *CLM* wave declines monotonically from 0.505699 at  $\theta_0 = 0$  to 0 at  $\theta_0 = 90$ .

When rotation is present (i.e. for  $\Omega^* = 0.1$  and  $0.2$ ), the amplitude ratio changes of all reflected waves are identical to those for  $\Omega^* = 0$  but the values of the amplitude ratio enhance for each incident angle.

## 6. Conclusions

This article examines how rotation affects the speed and amplitude ratio of reflected waves. By observing the graphical behaviour, the following significant conclusions can be drawn.

- (i) The value of speeds at each angle of incidence is altered by rotation, but the speed variation is unaffected.
- (ii) The order of the speeds of different plane waves is determined for the current numerical example as  $(v_{CLD} > v_{CTD} > v_{CLM} > v_{CTM})$ .
- (iii) With the increase in the rotation parameter value, the speeds of the *CLD* and *CTD* waves fluctuate, while those of the *CLM* wave fall and those of the *CTM* wave rise.
- (iv) As the value of the rotation parameter rises, the speeds of the *CLD* and *CTD* waves increase, whereas the speeds of the *CLM* wave and *CTM* wave decrease.

## Appendix

The formulas for  $p_j$ ,  $\frac{q_j}{k_j}$  and  $\frac{r_j}{k_j}$ ,  $j = 1, 2, \dots, 4$  are as follows:

$$p_j = \frac{A_{1j} + B_{1j}}{M_{1j} + N_{1j}}, \quad \frac{q_j}{k_j} = \frac{-i(A_{2j} + D_{2j})}{M_{1j} + N_{1j}}, \quad \frac{r_j}{k_j} = \frac{-i(A_{3j} + B_{3j})}{M_{1j} + N_{1j}},$$

where

$$A_{1j} = K_1 K_{1j}^* D_{33} \left[ 1 - \sin^2 \theta_0 \left( \frac{v_j}{v_1} \right)^2 \right]^{\frac{3}{2}} - K_{1j}^* K_2 D_{11} \sin^2 \theta_0 \left( \frac{v_j}{v_1} \right)^2 \sqrt{1 - \sin^2 \theta_0 \left( \frac{v_j}{v_1} \right)^2}, \quad j = 1, 2, \dots, 4,$$

$$B_{1j} = -R_j L_j D_{11} \sin \theta_0 \frac{v_j}{v_1} - P_j R_j D_{33} \sqrt{1 - \sin^2 \theta_0 \left( \frac{v_j}{v_1} \right)^2}, \quad j = 1, 2, \dots, 4,$$

$$M_{1j} = -K_2 K_{2j}^* D_{11} \sin^3 \theta_0 \left( \frac{v_j}{v_1} \right)^3 + K_1 K_{2j}^* D_{33} \sin \theta_0 \left( \frac{v_j}{v_1} \right) \sqrt{1 - \sin^2 \theta_0 \left( \frac{v_j}{v_1} \right)^2}, \quad j = 1, 2, \dots, 4,$$

$$N_{1j} = R_j Q_j D_{11} \sin \theta_0 \frac{v_j}{v_1} + R_j L_j D_{33} \sqrt{1 - \sin^2 \theta_0 \left( \frac{v_j}{v_1} \right)^2}, \quad j = 1, 2, \dots, 4,$$

$$A_{2j} = K_{1j}^* Q_j D_{11} \sin \theta_0 \left( \frac{v_j}{v_1} \right) \sqrt{1 - \sin^2 \theta_0 \left( \frac{v_j}{v_1} \right)^2} + K_{1j}^* L_j D_{33} \left[ 1 - \sin^2 \theta_0 \left( \frac{v_j}{v_1} \right)^2 \right], \quad j = 1, 2, \dots, 4,$$

$$B_{2j} = L_j K_{2j}^* D_{11} \sin^2 \theta_0 \left( \frac{v_j}{v_1} \right)^3 + P_j K_{2j}^* D_{33} \sin \theta_0 \left( \frac{v_j}{v_1} \right) \sqrt{1 - \sin^2 \theta_0 \left( \frac{v_j}{v_1} \right)^2}, \quad j = 1, 2, \dots, 4,$$

$$A_{3j} = K_1 K_{1j}^* Q_j \left[ 1 - \sin^2 \theta_0 \left( \frac{v_j}{v_1} \right)^2 \right] + K_{2j}^* K_2 P_j \sin^2 \theta_0 \left( \frac{v_j}{v_1} \right)^2, \quad j = 1, 2, \dots, 4,$$

$$B_{3j} = (K_1 K_{2j}^* + K_2 K_{1j}^*) L_j \sin \theta_0 \left( \frac{v_j}{v_1} \right) \sqrt{1 - \sin^2 \theta_0 \left( \frac{v_j}{v_1} \right)^2} + (L_j^2 - P_j Q_j) R_j, \quad j = 1, 2, \dots, 4,$$

$$P_j = \rho v_j^2 - A_{11} \sin^2 \theta_0 \left( \frac{v_j}{v_1} \right)^2 - A_{55} \left[ 1 - \sin^2 \theta_0 \left( \frac{v_j}{v_1} \right)^2 \right],$$

$$Q_j = \rho v_j^2 - A_{66} \sin^2 \theta_0 \left( \frac{v_j}{v_1} \right)^2 - A_{55} \left[ 1 - \sin^2 \theta_0 \left( \frac{v_j}{v_1} \right)^2 \right],$$

$$R_j = \rho v_j^2 - \frac{B_{77}}{j} \sin^2 \theta_0 \left( \frac{v_j}{v_1} \right)^2 - \frac{B_{66}}{j} \left[ 1 - \sin^2 \theta_0 \left( \frac{v_j}{v_1} \right)^2 \right] - \frac{\xi}{j k_j^2},$$

$$L_j = (A_{13} + A_{56}) \sin \theta_0 \left( \frac{v_j}{v_1} \right) \sqrt{1 - \sin^2 \theta_0 \left( \frac{v_j}{v_1} \right)^2},$$

$$K_{1j}^* = \frac{K_1}{j k_j^2}, \quad K_{2j}^* = \frac{K_2}{j k_j^2}.$$

## Acknowledgement

The author Princy Gupta gratefully acknowledges University Grants Commission (UGC), New Delhi for providing financial support through Basic Scientific Research (BSR) fellowship.

## Competing Interests

The authors declare that they have no competing interests.

## Authors' Contributions

All the authors contributed significantly in writing this article. The authors read and approved the final manuscript.

## References

- [1] M. Ciarletta, On the bending of microstretch elastic plates, *International Journal of Engineering Science* **37** (1999), 1309 – 1318, DOI: 10.1016/S0020-7225(98)00123-2.
- [2] A. C. Eringen, Theory of micropolar fluids, *Indiana University Mathematics Journal* **16** (1967), 1 – 18, DOI: 10.1512/iumj.1967.16.16001.
- [3] A. C. Eringen, Theory of thermo-microstretch elastic solids, *International Journal of Engineering Science* **28** (1990), 1291 – 1301, DOI: 10.1016/0020-7225(90)90076-U.

- [4] D. Iesan and A. Pompei, On the equilibrium theory of microstretch elastic solids, *International Journal of Engineering Science* **33** (1995), 399 – 410, DOI: 10.1016/0020-7225(94)00067-T.
- [5] A. Kiris and E. Inan, On the identification of microstretch elastic moduli of materials by using vibration data of plates, *International Journal of Engineering Science* **46** (2008) 585 – 597, DOI: 10.1016/j.ijengsci.2008.01.001.
- [6] R. Kumar, R. Singh and T. K. Chadha, Plane strain problem in microstretch elastic solid, *Sadhana* **28** (2003), 975 – 990, DOI: 10.1007/BF02703808.
- [7] M. Marin, A domain of influence theorem for microstretch elastic materials, *Nonlinear Analysis: Real World Applications* **11** (2010), 3446 – 3452, DOI: 10.1016/j.nonrwa.2009.12.005.
- [8] J. L. Nowinski, On the surface waves in an elastic micropolar and microstretch medium with nonlocal cohesion, *Acta Mechanica* **96** (1993), 97 – 108, DOI: 10.1007/BF01340703.
- [9] S. Sharma, K. Sharma and R. R. Bhargava, Plane waves and fundamental solution in an electro-microstretch elastic solids, *Afrika Matematika* **25** (2014), 483 – 497, DOI: 10.1007/s13370-013-0161-7.
- [10] J. N. Sharma, S. Kumar and Y. D. Sharma, Propagation of Rayleigh surface waves in microstretch thermoelastic continua under inviscid fluid loadings, *Journal of Thermal Stresses* **31** (2007), 18 – 39, DOI: 10.1080/01495730701737845.
- [11] B. Singh and M. Goyal, Wave propagation in a transversely isotropic microstretch elastic solid, *Mechanics of Advanced Materials and Modern Processes* **3** (2017), Article number: 8, DOI: 10.1186/s40759-017-0023-3.
- [12] D. Singh, N. Rani and S. K. Tomar, Dilatational waves at a microstretch solid/fluid interface, *Journal of Vibration and Control* **23**(20) (2017), 3448 – 3467, DOI: 10.1177/1077546316631158.

